

## Elucidating the interaction of letrozole with human serum albumin by combination of spectroscopic and molecular modeling techniques

Nooshin Bijari<sup>1,2</sup>, Sajad Moradi<sup>1</sup>, Sirous Ghobadi<sup>3</sup>, and Mohsen Shahlaei<sup>2,\*</sup>

<sup>1</sup>Nano Drug Delivery Research Center, Kermanshah University of Medical Sciences, Kermanshah, I.R. Iran.

<sup>2</sup>Medical Biology Research Center, Kermanshah University of Medical Sciences, Kermanshah, I.R. Iran.

<sup>3</sup>Department of Biology, Faculty of Science, Razi University, Kermanshah, I.R. Iran.

### Abstract

Human serum albumin (HSA) is the most abundant protein found in human blood and is extensively employed in clinical applications such as hypovolemic shock treatment. Also, there has been a lot of attempt to use HSA as a carrier to deliver various drugs to their specific targets. Thus, clarify of structure, dynamics, functions, and features of HSA-drug complexes play an important role from the viewpoint of pharmaceutical and/or biochemical sciences. In this study, the interaction of letrozole, as a non-steroidal aromatase inhibitor, with HSA has been studied by combining different techniques such as UV-Vis, fluorescence spectroscopy, and computational methods. The binding of letrozole quenches the serum albumin fluorescence intensities. A clear decrease in fluorescence intensities of letrozole-HSA complex with the increase in temperature showed the static mode of fluorescence quenching. The results of Stern-Volmer procedure analysis showed that letrozole is bound only to a site from the HSA. The results of thermodynamic analysis showed that reaction between HSA and letrozole is spontaneous and exothermic. Furthermore, by monitoring the intrinsic fluorescence and using site markers competitive measurement, the binding of letrozole in the neighborhood of Sudlow's site I of HSA has been proved. Finally, computational methods substantiated the experimental findings and it was revealed that letrozole was bound to Arg-209, Trp-214, Ala-350, and Gly-238 residues of subdomain IIA and IIIA of HSA, respectively.

**Keywords:** Human serum albumin; Fluorescence quenching; Letrozole; Site marker; Sudlow's site I.

### INTRODUCTION

According to epidemiological and experimental studies, estrogens are important factors in breast cancer and act through hormone-related pathways. Also, increasing of circulating level may lead to breast cancer in postmenopausal women (1). Aromatase is the final enzyme in steroid biosynthesis process that converts androgens to estrogens. Therefore, applying a selective inhibitor can block this step leading to inhibition of estrogens production. Modern third generation aromatase inhibitors (AIs) effectively inhibit the synthesis of estrogen via reversible competition mechanism inside aromatase binding site. AIs have been classified as steroidal (type I; for example, exemestane, formestane) or nonsteroidal (type II; for example, letrozole and anastrozole) (2,3).

Letrozole (LET) (4,4'-[1H-1,2,4-triazol-1-ylmethylene]-bis-benzonitrile) is a specific

nonsteroidal aromatase inhibitor suppressing estrogen biosynthesis that is administered orally in advanced breast cancer (4).

One of the most important factors affecting the distribution and concentration of administered drugs is the binding affinity for human serum albumin (HSA) (5). Human serum albumin transports various exogenous ligands such as drugs through blood circulation to specific target sites (6). Human serum albumin is a helical protein with a heart shape tertiary structure and approximate dimensions of  $8 \times 8 \times 3$  nm. It consists of three domains: domain I (residues 1-195), II (residues 196-383), and III (384-585) and in each domain there are two subdomains (A and B), and 17 disulfide bridges stabilizing the whole protein structure (7-11).

\*Corresponding author: M. Shahlaei  
Tel: +98-8334276489, Fax: +98-8334276493  
Email: m.shahlaei@kums.ac.ir

Access this article online



Website: <http://rps.mui.ac.ir>

DOI: 10.4103/1735-5362.235157

As a transport protein, HSA possesses several binding sites for structurally different ligands (12). Multiple binding sites enable HSA to interact with many organic and inorganic molecules. Therefore, HSA is an important regulator of pharmacokinetic behavior of many drugs (13). Due to the poor solubility of some anticancer drugs in aqueous solution, delivery of these drugs is a major challenge in cancer therapeutics. Therefore, the study of the interaction of drugs, exogenous molecules and biological molecules with albumin is very important and in recent years a large number of these studies have been reported in literature (7,9,14,15).

On the other hand, the study of the binding energy of medications with HSA, which is the most significant means of drug transplantation in the body, is very important from the pharmacokinetic point of view. The more robust interaction of a drug with a binding site can greatly hinder the interaction and thus the transfer of another drug that is attached to the same site and affects its therapeutic effects (16). That's why in these studies and as one of the most important results, number of binding sites along with interaction energies of drug-protein is examined (8,17-20). There are a lot of reports about interaction of drugs and HSA. Poureshghi and coworkers reported interaction of lamotrigine (an epileptic drug) with HSA by fluorescence, UV-Vis, Fourier-transform infrared spectroscopy (FTIR), circular dichroism (CD) spectroscopic techniques, and molecular modeling methods (21). Ajmal, *et al.* investigated the binding interaction between clofarabine, an important anticancer drug, and two important carrier proteins found abundantly in human plasma, HSA and  $\alpha$ -1 acid glycoprotein (AAG), by spectroscopic and molecular modeling methods (22). Maryam, *et al.* published a study to characterize the mechanism of doripenem binding and to locate its site of binding on HSA by using spectroscopic and docking approaches (23).

The recent published studies showed that the anticancer drugs, such as doxorubicin, tamoxifen and its metabolites could be transported by human serum proteins. The interaction of tamoxifen and its metabolites

with HSA can be used as a model for elucidating the nature of tamoxifen binding with the estrogen receptor, and to gain insight into the mechanism of action of tamoxifen in breast cancer therapy (24). In this report, interaction of HSA with LET has been discussed by various experimental methods such as UV-Vis, fluorescence spectroscopy, as well as computational modeling analysis. Therefore, the binding characteristics of LET to HSA is studied in terms of the binding affinity, interaction forces, location of the binding site, and structural changes in HSA upon LET binding.

## MATERIALS AND METHODS

### Materials

Human serum albumin and LET were purchased from Sigma Chemical Company (St. Louis, USA). A stock solution of HSA was prepared as follows: a known amount of HSA was dissolved in a fixed volume of 0.1 M phosphate buffer, pH 7.5. It must be noted that the HSA final concentration was determined spectrophotometrically using a molar extinction coefficient of  $35,700 \text{ M}^{-1} \text{ cm}^{-1}$  at 280 nm (25) and molecular weights of 66,000 Da (26). The stock solution ( $1.0 \text{ mg mL}^{-1}$ ) of drug was prepared in dimethyl sulphoxide (DMSO). In all measurements, the final concentration of DMSO remained less than 1% (v/v). All other chemicals were of analytical reagent grade. Double distilled and deionized water was used in all experiments.

### Spectral measurements

#### Fluorescence quenching

Fluorescence spectra were recorded using a spectrofluorimeter Model Cary Eclipse (Varian, Australia) equipped with a 150 W xenon lamp. Fluorescence quenching has also been used for studying the interaction of LET with HSA. In each spectrum recording, different concentrations of LET were mixed with  $3 \mu\text{M}$  HSA in a 1-cm path length quartz cuvette (3.0 mL). The fluorescence experiments were carried out in the wavelength range of 305-450 nm. The excitation wavelength used for all experiments was 295 nm after 1 min incubation at room temperature.

### Correction of the inner filter effect

Following equation was used for correcting inner filter effect in the fluorescence data:

$$F_{\text{corr}} = F_{\text{obs}} \text{ anti log}[(A_{\text{em}} + A_{\text{ex}}) / 2] \quad (1)$$

where,  $F_{\text{corr}}$  and  $F_{\text{obs}}$  are the corrected and observed fluorescence intensity, respectively.  $A_{\text{ex}}$  and  $A_{\text{em}}$  are the absorbances of the sample at the excitation (295) and emission (305-450) wavelengths, respectively (27).

### Quenching mechanism

Fluorescence spectroscopy also was used for determining the quenching mechanism as well as major binding forces at the different temperatures (*i.e.* 298, 303, 308, and 313 K) (28). The well-known Stern-Volmer equation (following equation) was employed to study the quenching mechanism (the decrease in fluorescence intensities at  $\lambda_{\text{max}}$ ) involved in the interaction of LET with HSA.

$$F_0 / F = 1 + k_q \tau_0 [Q] = 1 + K_{\text{SV}} [Q] \quad (2)$$

where,  $F_0$  and  $F$  are the fluorescence intensities of the protein in the absence and the presence of the ligand (drug), respectively;  $[Q]$  is the concentration of the ligand and  $K_{\text{SV}}$  is the Stern-Volmer quenching constant (29). Following equation was used for determining the values of the bimolecular quenching rate constant ( $k_q$ ) for LET-HSA system:

$$k_q = k_{\text{sv}} / \tau_0 \quad (3)$$

where,  $\tau_0$  is the average life time of the fluorophore in the absence of the drug (30). Following double logarithmic equation also was used for determining the values of the binding constant ( $K_b$ ) for the LET-HSA system:

$$\log \{(F_0 - F) / F\} = \log K_b + n \log [Q] \quad (4)$$

where,  $K_b$  and  $n$  are the binding constant and the average number of binding sites per HSA, respectively. Thus, a plot of  $\log (F_0 - F) / F$  versus  $\log [Q]$  can be used to determine  $K_b$  as well as the  $n$  (31).

### Thermodynamic analysis of the binding process

Thermodynamic analysis was investigated for determining parameters like enthalpy

change ( $\Delta H^\circ$ ), entropy change ( $\Delta S^\circ$ ) and the Gibbs free energy change ( $\Delta G^\circ$ ). These parameters were used for characterizing the acting forces involved in the binding phenomenon. The well-known van't Hoff equation was used for determining the values of  $\Delta H^\circ$  and  $\Delta S^\circ$ :

$$\ln K_b = -(\Delta H^\circ / RT) + (\Delta S^\circ / R) \quad (5)$$

where,  $R$  is the gas constant ( $8.314 \text{ J mol}^{-1} \text{ K}^{-1}$ ) and  $T$  is the temperature (32).

The values of  $\Delta S^\circ$  and  $\Delta H^\circ$  can be calculated from the y-intercept and slope of the van't Hoff plot, respectively. In addition, the following equation (Gibbs equation) was used for the free energy change ( $\Delta G^\circ$ ) (33):

$$\Delta G^\circ = \Delta H^\circ - T\Delta S^\circ \quad (6)$$

### Competitive site marker displacement experiments

Competitive experiments for site marker displacement were used to locate binding site of LET on HSA. Two site markers, used in these experiments were warfarin and ibuprofen for sites I and II, respectively (34). Competitive site marker displacement experiments were carried out by titrating  $3 \mu\text{M}$  HSA and its equimolar complexes with site markers while LET concentration was increased continuously. The mixture of site marker and HSA was allowed to equilibrate for 1 h at room temperature before titration. All experiments and recordings were carried out at room temperature. Also, for exciting of HSA and recording emission spectra, the instrument was set at 295 nm.

### Docking studies and molecular dynamics simulation

To clarify the atomistic details of binding mechanism of LET to the HSA and provide computational evidence to experimental results, molecular docking and molecular dynamics simulation were applied. The AutoDock 4.2 software was used to perform molecular docking of LET and HSA (35). Human serum albumin structure was obtained from the RCSB protein data bank (1AO6) (<http://www.rcsb.org>) (36). The LET two dimensional structure was sketched by ACD/LAB (<http://www.acdlabs.com>) followed

by preparing and optimizing of three dimensional structure using the HyperChem 8.0.6 program (37) (Fig. 1). The optimized structure of LET, provided by a semiempirical method of Austin model 1 (AM1) was used as input for AutoDockTools (38). All rotatable bonds for ligand were set up as active and gasteiger charges were assigned to the protein. A box of 126, 126, 126, points with grid spacing of 0.7 Å was accessible to AutoGrid to search and create the atomic energy maps of all atom types (39). The most suitable conformations of LET-HSA, in terms of cluster population with the acceptable bonding energy, were selected for molecular dynamics studying. The LigPlot program (<http://www.ebi.ac.uk>) and AutoDockTools 1.5.4 (35) were applied to show the residues around ligand and analyze the interaction mode such as binding sites between LET and HSA. Molecular graphics were prepared by VMD version 1.8.9 (40). All molecular dynamics (MD) simulations were carried out using the GROMACS simulation package version 5.0.1 with GROMACS 53a6 force field, on an Intel Core i7 extreme edition under Ubuntu Linux (41). The structure of complex of LET and HSA obtained from the docking procedure was used as starting point for the MD simulation. Topology parameter for LET was obtained from Automated Topology Builder (ATB) server (<https://atb.uq.edu.au/>). Human serum albumin and HSA-LET complex were centered in an 11.11.11 nm<sup>3</sup> cubic box and then solvated with 44470 of SPCE water molecules and simulated using periodic boundary conditions. The system then neutralized by using 15 atom of NA and was subjected to energy minimization until the maximum forces were reached below 500kJ/mol<sup>1</sup>. Using Berendsen thermostat, the temperature was kept constant at 300 K in all simulations (42) and pressure was set close to 1 bar by the Parrinello-Rahman barostat respectively in NVT and NPT ensembles (43). All bonds were constrained in normal lengths under the linear constraint solver (LINCS) method. Electrostatic non-bonded interactions using the particle mesh Ewald (PME) method, van der Waals forces using lennard-jones function were calculated within cut off of 10Å (7). Finally a production molecular dynamics of 50 ns was performed on LET-HSA complex using leap-frog algorithm (44).

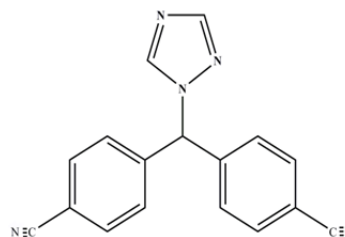


Fig. 1. Chemical structure of letrozole.

## RESULTS

### Fluorescence analysis

#### Fluorescence quenching of HSA by letrozole

As shown in Fig. 2, the protein has an emission maximum at about 343 nm, which is attributed to the presence of lone tryptophan (Trp-214) residue at subdomain IIA. As can be seen, the fluorescence emission spectra of serum albumin in the presence of different amounts of LET were recorded in the range of 305 - 450 nm upon excitation at 295 nm.

#### Fluorescence quenching mechanism

Based on equation 2, we can analyze the fluorescence quenching obtained at four temperatures of 298, 303, 308, and 313 K (2). Using these data, useful plots can be generated called "Stern-Volmer plots" as shown in Fig. 3. The linearity of the  $F_0 / F$  versus  $[Q]$  plots for HSA revealed the quenching type, the static or dynamic, since the characteristic Stern-Volmer plot of combined quenching (simultaneously static and dynamic) is an upward curvature (45). Values of  $K_{SV}$  and  $k_q$  at various temperatures were obtained from Fig. 3 and are listed in Table 1 (17).

#### Binding modes and number of binding sites

Figure 4 shows double logarithmic plots for the binding of LET to HSA at different temperatures, as obtained after treatment of the fluorescence quenching data according to equation 4. The  $K_b$  measured at different temperatures is summarized in Table 1. The value of  $n$  is close to 1 and the binding constant decrease with increasing temperature. Since the  $K_b$  value for the LET-HSA system was found to remain in the range of  $1.70-1.25 \times 10^4 \text{ M}^{-1}$ , it indicated a moderate binding affinity between LET and HSA. Such moderate binding affinity is beneficial for the efficient transport of the drug and its subsequent release at its target site (46).

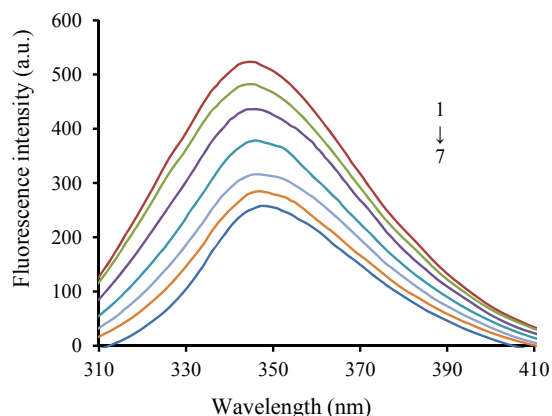


**Fig. 2.** The intrinsic fluorescence spectra of human serum albumin in the (1) absence and (2) presence of 100, (3) 200, (4) 400, (5) 600, (6) 800, and (7) 100  $\mu$ M letrozole. Human serum albumin (5  $\mu$ M) was excited at 295 nm.

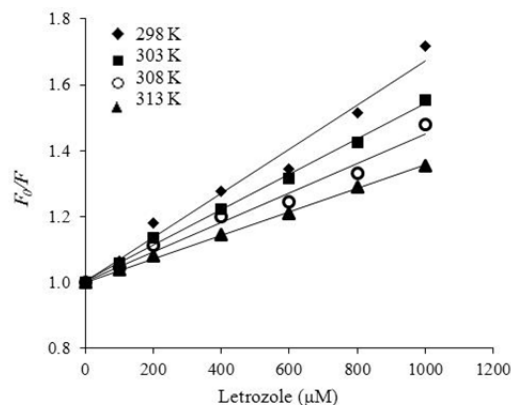


**Fig. 3.** The Stern–Volmer plots for human serum albumin (HSA) fluorescence quenching upon letrozole binding at 298, 303, 308, and 313 K. The HSA concentration was 5  $\mu$ M in 0.1 M phosphate buffer, pH 7.5.  $F_0/F$ , relative fluorescence intensity.

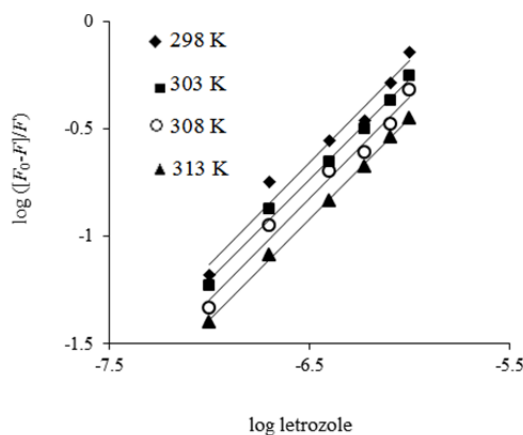


**Fig. 4.** The modified Stern-Volmer plots for fluorescence quenching of human serum albumin (HSA) upon letrozole binding at 298, 303, 308, and 313 K. The HSA concentration was 5  $\mu$ M in 0.1 M phosphate buffer, pH 7.5.  $F_0/F$ , relative fluorescence intensity.

**Table 1.** The Stern-Volmer quenching constant ( $K_{SV}$ ), bimolecular quenching rate constant ( $K_q$ ) and binding constant ( $K_b$ ) for binding of letrozole to human albumin serum (HSA) at different temperatures.

Complex	Parameters						
	T (K)	$K_{sv} \times 10^{-4}$ ( $M^{-1}$ )	$K_q \times 10^{-12}$ ( $M^{-1} s^{-1}$ )	$K_b \times 10^{-4}$ ( $M^{-1}$ )	$\Delta S^\circ$ ( $J mol^{-1} K^{-1}$ )	$\Delta H^\circ$ ( $kJ mol^{-1}$ )	$\Delta G^\circ$ ( $kJ mol^{-1}$ )
HSA-Drug	298	$67.47 \pm 0.13$	$67.47 \pm 0.13$	$31.62 \pm 0.58$	$-13.85 \pm 1.14$	$-35.33 \pm 2.41$	$-31.20 \pm 0.62$
	303	$54.56 \pm 0.46$	$54.56 \pm 0.46$	$20.23 \pm 1.61$			$-31.13 \pm 0.30$
	308	$45.18 \pm 0.59$	$45.18 \pm 0.59$	$19.14 \pm 0.15$			$-31.06 \pm 0.14$
	313	$35.84 \pm 1.06$	$35.84 \pm 1.06$	$14.62 \pm 0.54$			$-30.99 \pm 0.59$

Data are expressed as mean  $\pm$  SD of three measurements.

**Determination of thermodynamic parameters**

Values of  $\Delta H^\circ$  and  $\Delta S^\circ$ , as obtained from the slope and the intercept, respectively, of the Van't Hoff plot along with the  $\Delta G^\circ$  values at four different temperatures are listed in Table 1. When we applied this analysis to the

binding system of drug and HSA, we found that  $\Delta H^\circ < 0$  and  $\Delta S^\circ < 0$ .

**Site marker competitive experiments**

Binding location studies between HSA and LET in the presence of two site markers

(warfarin, as site I marker and ibuprofen, as site II marker) were measured using the fluorescence titration method. Letrozole was added to solutions of HSA and site markers held in equimolar concentrations ( $3.0 \times 10^{-6}$  M), pH 7.5, for 1 h. The relative fluorescence intensity  $F/F_0$  versus ligand concentration plots is displayed in Fig. 5. The fluorescence quenching data of the HSA-LET system with the presence of site markers were analyzed using equation 4. The binding constants for HSA-LET complex in the absence of site markers, in the presence of warfarin and ibuprofen, were determined as  $36.84 \pm 1.02 \times 10^{-4}$ ,  $17.58 \pm 0.53 \times 10^{-4}$ , and  $31.2 \pm 0.95 \times 10^{-4}$  ( $M^{-1}$ ), respectively.

### Molecular docking

In order to get more information about binding sites of LET on HSA, molecular docking was employed to simulate LET and

HSA interaction. The best energy ranked results are shown in Fig. 6. The docking results implied that LET binds within the binding pocket of subdomain IIA. As illustrated in Fig. 6, Trp-214 residues were close to LET. This finding gives a reliable proof to clarify the efficient fluorescence quenching of HSA emission in the presence of LET.

The main residues involved in the interaction were generated using LigPlot v.1.4 and depicted in Fig. 7. The LET molecule is located within the subdomain II adjacent to Leu-331, Arg-209, Val-216, Ala-350, Ala-231, Glu-354, Asp-324, Gly-328, and Lys-351 residues. Schematic representation of LET in Sudlow's site I is shown in Fig. 8. In the other hand, docking results indicate that H-bonding and van der Waals forces are dominant forces involved in the interaction that is in full agreement with experimental ones.

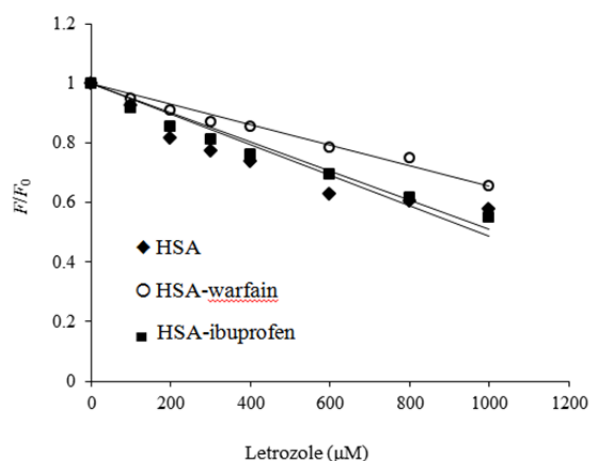


**Fig. 5.** Fluorescence quenching profiles of human serum albumin (HSA), and HSA-warfarin, and HSA-ibuprofen in the presence of various concentration of letrozole.  $F_0/F$ , relative fluorescence intensity.



**Fig. 6.** Crystal structure of human serum albumin (HSA) and the positions of single tryptophan residue (Trp214) and also the binding site of letrozole (LET) in HSA (after docking). Protein backbone is shown in the “cartoon” representation, LET and Trp214 residue in the site I are shown in the “stick” representation. The LET and Trp214 structures are represented by the red and blue colors, respectively.

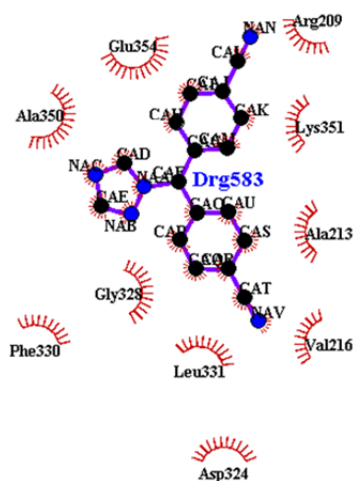


**Fig. 7.** Two dimensional schematic representations of human serum albumin-letrozole. Drawings were generated using LigPlot v.1.4 (after docking).

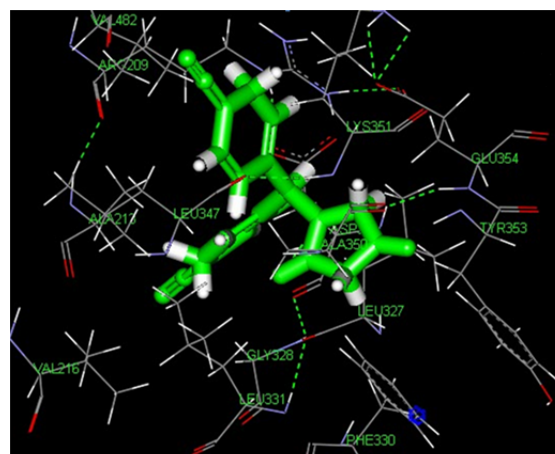


**Fig. 8.** Schematic representation of letrozole in Sudlow's site I (after docking). (For interpretation of references to color in this figure legend, the reader is referred to the web version of this paper.)

**Table 2.** Docking results of LET to different binding sites of HSA

Binding site	Parameters		
	Number in cluster	Mean binding energy	Lowest binding energy
Warfarin site	110	-6.49	-6.94
Ibuprofen site	20	-4.32	-4.8

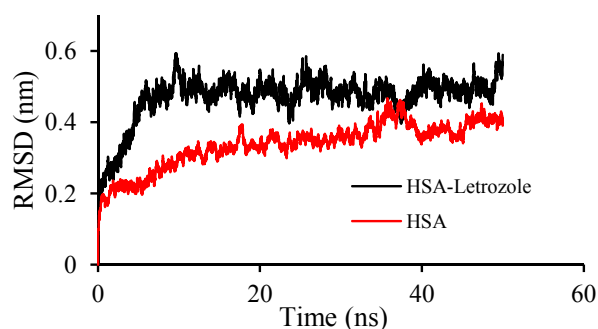


**Fig. 9.** Time dependencies of the root mean square deviation (RMSD) (nm) of human serum albumin (HSA) and HSA-letrozole complex systems. (For interpretation of references to color in this figure legend, the reader is referred to the web version of this paper).

Other important result from docking analysis is a bout preference of LET to different binding sites of ibuprofen and warfarin (Table 2). Obtained data indicate perfect tendency of LET to warfarin site than ibuprofen site either in number in cluster and binding energy. These results are in good agreement with laboratory experiments. The calculation of the nature of the forces involved in the interaction is also done using the Discovery Studio (version 2.5) and the results indicate that they are in line with other data

obtained at docking. The energy of the interaction calculated here was -11 kcal/mol, which were -9.8 for the van der Waals forces.

#### **Molecular dynamics simulation**

One of the most important measure of the stability and conformational drift of a typical protein in a molecular simulation is provided by the root mean square deviation (RMSD) of the protein coordinates from the initial values as a function of time of simulation (Fig. 9). In the last 10 ns simulation, the whole  $C_{\alpha}$  of HSA

is fairly stable as indicated by the small magnitude of RMSD fluctuation of the system. Also the RMSD value for complex system is a bit more than those of free HSA that may be due to the more interaction of HSA atoms in the presence of LET that results some conformational and structural changes. To provide a more detailed description of the flexibility of the protein residues, the root mean square fluctuations (RMSF) of all residues of HSA, in the absence and presence of the drug, were then calculated (Fig. 10). This figure clearly depicts different flexibilities in the binding pocket of HSA in the presence and absence of LET. The LET binding site (Glu-208-Arg-222, Asp-324-Arg-337, and Val-343-leu-357, the regions are specified with three bars) show relative small degree of flexibility upon LET-HSA interaction, indicating that residues locating in the drug binding site seem to be more rigid as a result of binding to LET, which is in perfect agreement with the RMSD results. The results of the H-bond analysis showed that the number of hydrogen bonds reach to a

maximum of 5 and have an average of 3 during simulation time (Fig 11). The changes in center of mass of the LET with the HSA are calculated over time, and the results are shown in (Fig 12). As can be seen, after a 1 Å decrease in the first picoseconds of simulation it is fixed in about 1.6 Å.

The effects of LET binding on changes in the number of amino acids present in the protein secondary structures were investigated by DSSP analysis. The results showed that the average of this number in free protein during the simulation was 430. This value was reduced by the binding of the LET to 425, which indicates very low levels of structural changes in the protein occurred due to drug interactions that is in agreement with other results.

A comparison study between the different constants of this study with a few published interactions of drugs with HSA is reported in Table 3. As it can be seen, the different constants of LET calculated in this study are comparable to some of the previous reports (Table 3).

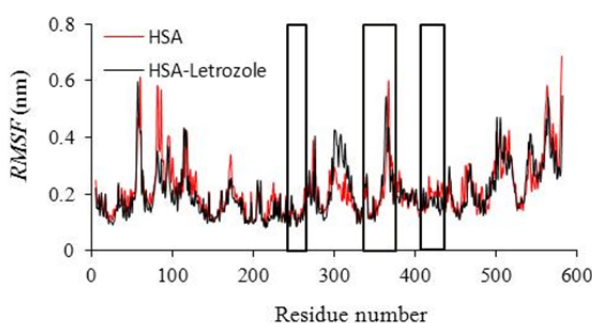


**Fig. 10.** The root mean square deviation (RMSD) of human serum albumin (HSA) and HSA-letrozole complex. The residues located in binding pocket specified by two bars. (For interpretation of references to color in this figure legend, the reader is referred to the web version of this paper).

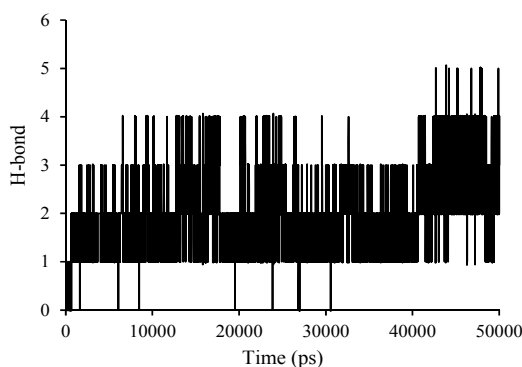


**Fig. 11.** The H-bonding analysis for letrozole and human serum albumin (HSA) interaction during simulation time.



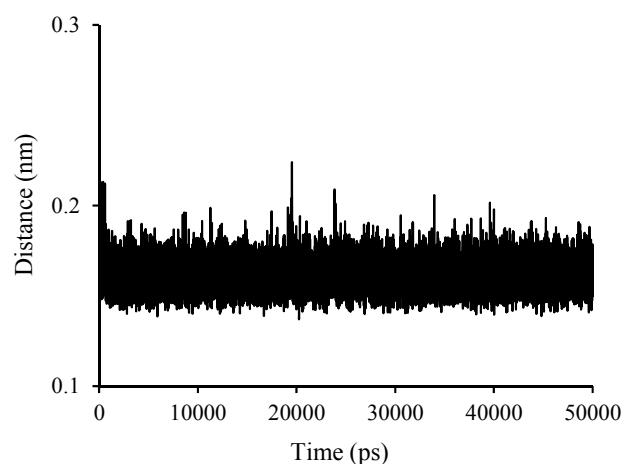


**Fig. 12.** Time dependent changes in center of masses between letrozole and human serum albumin (HSA).

**Table 3.** A comparison of different parameters of interaction of letrozole with human serum albumin (HSA) to the reported papers.

Drug	Parameters				Reference
	$K_{sv} \times 10^{-4}$ ( $M^{-1}$ )	$K_q \times 10^{-12}$ ( $M^{-1} s^{-1}$ )	$K_b \times 10^{-5}$ ( $M^{-1}$ )	Number of binding sites (n)	
Vitamin B12	4.33	4.33	6.93	1.34	(17)
Salvianolic acid B	4.79	4.79	1.84	1.05	(18)
Paraquat	3.95	3.95	48.53	1.02	(19)
Indomethacin	14.46	14.46	361.40	1.45	(8)
Ibuprofen	0.065	0.065	16.4	1.11	(8)
Carbamazepine	1.27	1.27	20.81	1.01	(20)

## DISCUSSION

Interaction of protein with a drug could affect its molecular, biological activity, and functioning. Therefore, studying the interaction has great importance. Most drugs administered to the body could bind to serum albumin and the binding information plays an important role in medicine (47). Letrozole causes a concentration dependent quenching of the intrinsic fluorescence with HSA. These results indicated that there were interactions between LET and HSA and the binding reactions resulted in non-fluorescent complex (26). The regular decrease of emission signal of the protein without changing the shape of the peaks may imply that the tryptophan residue should be located at or near the drug-binding site (7-10,30,34). The results of Stern-Volmer plot indicated that the value of  $K_{sv}$  decreased with increasing temperature in the presence of LET demonstrating that the quenching mechanism is static. On the other hand, the maximum scatter collision

quenching constant reported for various kinds of quencher to a biopolymer ( $k_q$ ) is  $2.0 \times 10^{10} M^{-1} s^{-1}$ . The  $k_q$  values are greater than the maximum scatter collision quenching indicating that the quenching mechanism involved in the LET-HSA system was initiated by static rather than dynamic quenching process (48). The value of  $K_b$  is significant to understand the distribution of the drug in plasma since the weak binding can lead to a short lifetime or poor distribution, while strong binding can decrease the concentration of free drug in plasma (7-10). Since the  $K_b$  value for the LET-HSA system was found to be in the range of  $1.70-1.25 \times 10^4 M^{-1}$ , a moderate binding affinity between LET and has could be assumed. Such moderate binding affinity is beneficial for the efficient transport of the drug and its subsequent release at its target site (46). The dependence of binding constant on temperature indicates that a thermodynamic process is responsible for the formation of the complex. This dependence was therefore, analyzed in order to better characterization of

the forces acting between ligand and protein. According to the  $\Delta H^\circ$  and  $\Delta S^\circ$  data, the mode of interaction between the drug and the biomolecule can be inferred. The negative values of  $\Delta H^\circ$  and  $\Delta S^\circ$  indicate that the binding of the investigated drug to the HSA proceeds predominantly via van der Waals interactions and hydrogen bonds. In addition, the high negative value of  $\Delta H^\circ$  revealed that the formation of LET-HSA complex was an enthalpy driven. The negative sign of  $\Delta G^\circ$  value showed spontaneous nature of the binding reaction at all temperatures (49). A fundamental characteristic of HSA is its surprising capacity to bind a large variety of drugs (50). Taking into account the high concentration of HSA in plasma, the binding affinity of drugs to HSA is an important factor to be considered when designing and developing new drugs. Since HSA has a limited number of high affinity binding sites, detailed molecular information about these sites could be helpful in the assessment of cooperative effects during the binding of other drugs or endogenous ligands (51). Analysis of the binding constants of site markers indicated that the binding constant was changed obviously by warfarin, while ibuprofen slightly changed this constant. Site I (subdomain IIA) has been proposed as the LET binding site in HSA based on competitive ligand displacement experiments. These results clearly suggested site I as the preferred LET binding site on HSA. Furthermore, these results were in line with our molecular docking analysis. As illustrated in molecular docking studies, LET molecule was located within the binding pocket of site I and its rings were not coplanar. The benzene rings of LET were inserted in the hydrophobic cavity formed by Val-482, Arg-209, Leu-347, Ala-213, Val216, and the triazole moiety was suited in a less hydrophobic cavity formed by Arg-351, Glu-354, Ala-350, Tyr-353, Leu-327, Asp-324, and Gly-328. In addition, it was also important to note that the polar residues (such as Arg-209, Lys-351, Tyr-353, Glu-354, and Asp-324) in the proximity to LET play a subordinate role in stabilizing the drug molecule via hydrogen bonding. The results have shown that LET can interact with

HSA at the interface between subdomains IIA and IIB (in close proximity to the site I) through hydrophobic interactions as well as hydrogen bonding, which is consistent with the thermodynamic parameters obtained from fluorescence quenching experiments. The aim of the MD simulation study was to get more precise drug-HSA models in a state close to the natural / real conditions and to explore the binding modes of the drug further. Although molecular docking offers reasonable binding structures for LET, the MD simulation can account for even the smallest variances (7,9). Average RMSD of the HSA-LET complex is higher than that of the HSA and indicates an increased flexibility of the protein backbone because of protein complexation which was in good agreement with RMSF.

## CONCLUSION

This paper provided an approach for studying the interactions of fluorescent protein with LET using different spectroscopic methods and molecular modeling techniques. Protein binding, especially binding to HSA, is one of the most important issues to be considered for each drug because it determines the pharmacokinetics, elimination half-time, and availability of the drug in various tissues. The main objective of this study was characterizing the main nature of the binding *in vitro* under a simulated physiological condition and understanding the effect of the binding of LET on conformational changes of HSA. This report could be valuable due to the importance of LET in the treatment of advanced breast cancer and significance in pharmacology and clinical outcome of the drug.

## ACKNOWLEDGMENT

This work was financially supported (Grant No. 95302) by the Kermanshah University of Medical Sciences Research Council, Kermanshah, I.R. Iran.

## REFERENCES

1. Travis RC, Key TJ. Oestrogen exposure and breast cancer risk. *Breast Cancer Res.* 2003;5(5):239-247.

2. Bhatnagar AS. The discovery and mechanism of action of letrozole. *Breast Cancer Res Treat.* 2007;105(Suppl 1):7-17.
3. Mojaddami A, Sakhteman A, Fereidoonzhad M, Faghih Z, Najdian A, Khahnadideh S, et al. Binding mode of triazole derivatives as aromatase inhibitors based on docking, protein ligand interaction fingerprinting, and molecular dynamics simulation studies. *Res Pharm Sci.* 2017;12(1):21-30.
4. Colussi DM, Parisot CY, Lefèvre GY. Plasma protein binding of letrozole, a new nonsteroidal aromatase enzyme inhibitor. *J Clin Pharmacol.* 1998;38(8):727-735.
5. Ghuman J, Zunszain PA, Petitpas I, Bhattacharya AA, Otagiri M, Curry S. Structural basis of the drug-binding specificity of human serum albumin. *J Mol Biol.* 2005;353(1):38-52.
6. Kabir MZ, Tee WV, Mohamad SB, Alias Z, Tayyab S. Interaction of an anticancer drug, gefitinib with human serum albumin: insights from fluorescence spectroscopy and computational modeling analysis. *RSC Adv.* 2016;6(94):91756-91767.
7. Shahlaei M, Rahimi B, Ashrafi-Kooshk MR, Sadrjavadi K, Khodarahmi R. Probing of possible olanzapine binding site on human serum albumin: Combination of spectroscopic methods and molecular dynamics simulation. *J Lumin.* 2015;158:91-98.
8. Moradi N, Ashrafi-Kooshk MR, Ghobadi S, Shahlaei M, Khodarahmi R. Spectroscopic study of drug-binding characteristics of unmodified and pNPA-based acetylated human serum albumin: Does esterase activity affect microenvironment of drug binding sites on the protein?. *J Lumin.* 2015;160:351-361.
9. Shahlaei M, Rahimi B, Nowroozi A, Ashrafi-Kooshk M R, Sadrjavadi K, Khodarahmi R. Exploring binding properties of sertraline with human serum albumin: Combination of spectroscopic and molecular modeling studies. *Chem Biol Interact.* 2015;242:235-246.
10. Jafari F, Samadi S, Nowroozi A, Sadrjavadi K, Moradi S, Ashrafi-Kooshk MR, et al. Experimental and computational studies on the binding of diazinon to human serum albumin. *J Biomol Struct Dyn.* 2018;36(6):1490-1510.
11. Soheili V, Abdollahpour N, Zendeabad S, Abdollahpour M, Alipour A. Bioinformatics analysis of human serum albumin for determination of herbal anti-diabetic compound binding site. *Res Pharm Sci.* 2012;7(5):S519.
12. Beiranvand Z, Bani F, Kakanejadifard A, Laurini E, Fermeglia M, Pricl S, et al. Anticancer drug delivery systems based on specific interactions between albumin and polyglycerol. *RSC Adv.* 2016;6(14):11266-11277.
13. Tajmir-Riahi HA. An overview of drug binding to human serum albumin: protein folding and unfolding. *Sci Iran.* 2007;14(2):87-95.
14. Moradi N, Ashrafi-Kooshk MR, Chamani J, Shackebaei D, Norouzi F. Separate and simultaneous binding of tamoxifen and estradiol to human serum albumin: Spectroscopic and molecular modeling investigations. *J Mol Liq.* 2018;249:1083-1096.
15. Moradi S, Taran M, Shahlaei M. Investigation on human serum albumin and Gum Tragacanth interactions using experimental and computational methods. *Int J Biol Macromol.* 2018; 107(Pt B):2525-2533.
16. Yamasaki K, Chuang VT, Maruyama T, Otagiri M. Albumin-drug interaction and its clinical implication. *Biochim Biophys Acta.* 2013;1830(12):5435-5443.
17. Hou HN, Qi ZD, OuYang YW, Liao FL, Zhang Y, Liu Y. Studies on interaction between Vitamin B12 and human serum albumin. *J Pharm Biomed Anal.* 2008;47(1):134-139.
18. Chen T, Cao H, Zhu S, Lu Y, Shang Y, Wang M, et al. Investigation of the binding of Salviaolic acid B to human serum albumin and the effect of metal ions on the binding. *Spectrochim Acta A Mol Biomol Spectrosc.* 2011;81(1):645-652.
19. Zhang G, Wang Y, Zhang H, Tang S, Tao W. Human serum albumin interaction with paraquat studied using spectroscopic methods. *Pest Biochem Phys.* 2007;87(1):23-29.
20. Kalanur SS, Seetharamappa J, Kalalbandi VK. Characterization of interaction and the effect of carbamazepine on the structure of human serum albumin. *J Pharm Biomed Anal.* 2010;53(3):660-666.
21. Poureshghi F, Ghandforoushan P, Safarnejad A, Soltani S. Interaction of an antiepileptic drug, lamotrigine with human serum albumin (HSA): Application of spectroscopic techniques and molecular modeling methods. *J Photochem Photobiol B.* 2017;166:187-192.
22. Ajmal MR, Nusrat S, Alam P, Zaidi N, Khan MV, Zaman M, et al. Interaction of anticancer drug clofarabine with human serum albumin and human  $\alpha$ -1 acid glycoprotein. Spectroscopic and molecular docking approach. *J Pharm Biomed Anal.* 2017;135:106-115.
23. Maryam L, Sharma A, Azam MW, Khan SN, Khan AU. Understanding the mode of binding mechanism of doripenem to human serum albumin: Spectroscopic and molecular docking approaches. *J Mol Recognit.* 2018:e2710. DOI: 10.1002/jmr.2710.
24. Bourassa P, Thomas TJ, Tajmir-Riahi HA. A short review on the delivery of breast anticancer drug tamoxifen and its metabolites by serum proteins. *J Nanomed Res.* 2016;4(2):80-87.
25. Chatterjee T, Pal A, Dey S, Chatterjee BK, Chakrabarti P. Interaction of virstatin with human serum albumin: spectroscopic analysis and molecular modeling. *PLoS One.* 2012;7(5):e37468-e37479.
26. Kandagal PB, Ashoka S, Seetharamappa J, Shaikh SMT, Jadegoud Y, Ijare O. Study of the interaction of an anticancer drug with human and bovine serum albumin: Spectroscopic approach. *J Pharm Biomed Anal.* 2006;41(2):393-399.
27. Yeggoni DP, Kuehne C, Rachamalla A, Subramanyam R. Elucidating the binding interaction

- of andrographolide with the plasma proteins: biophysical and computational approach. *RSC Adv.* 2017;7(79):5002-5012.
28. Bai HX, Liu XH, Yang F, Yang XR. Interactions of human serum albumin with phenothiazine drugs: insights from fluorescence spectroscopic studies. *J Chin Chem Soc.* 2009;56(4):696-702.
  29. Alam P, Chaturvedi SK, Anwar T, Siddiqi MK, Ajmal MR, Badr G, *et al.* Biophysical and molecular docking insight into the interaction of cytosine  $\beta$ -D arabinofuranoside with human serum albumin. *J Lumin.* 2015;164:123-130.
  30. Bijari N, Ghobadi S, Mahdiuni H, Khodarahmi R, Ghadami SA. Spectroscopic and molecular modeling studies on binding of dorzolamide to bovine and human carbonic anhydrase II. *Inter J Biol Macromol.* 2015;80:189-199.
  31. Shen GF, Liu TT, Wang Q, Jiang M, Shi JH. Spectroscopic and molecular docking studies of binding interaction of gefitinib, lapatinib and sunitinib with bovine serum albumin (BSA). *J Photochem Photobiol B.* 2015;153:380-390.
  32. Xu H, Yao N, Xu H, Wang T, Li G, Li Z. Characterization of the interaction between eupatorin and bovine serum albumin by spectroscopic and molecular modeling methods. *Int J Mol Sci.* 2013;14(7):14185-14203.
  33. Chaturvedi SK, Ahmad E, Khan JM, Alam P, Ishtikhar M, Khan RH. Elucidating the interaction of limonene with bovine serum albumin: a multi-technique approach. *Mol Biosyst.* 2015;11(1):307-316.
  34. Bijari N, Shokoohinia Y, Ashrafi-Kooshk MR, Ranjbar S, Parvaneh S, Moieni-Arya M, *et al.* Spectroscopic study of interaction between osthole and human serum albumin: Identification of possible binding site of the compound. *J Lumin.* 2013;143:328-336.
  35. Morris GM, Huey R, Lindstrom W, Sanner MF, Belew RK, Goodsell DS, *et al.* AutoDock4 and AutoDockTools4: Automated docking with selective receptor flexibility. *J Comput Chem.* 2009;30(16):2785-2791.
  36. Berman HM, Westbrook J, Feng Z, Gilliland G, Bhat TN, Weissig H, *et al.* The Protein Data Bank, 1999-. In: Fuess H, Hahn Th, Wondratschek H, Müller U, Shmueli U, Prince E, *et al.*, editors. *International Tables for Crystallography. Vol F: Crystallography of Biological Macromolecules.* Springer; 2006. pp. 675-684.
  37. Froimowitz M. HyperChem: a software package for computational chemistry and molecular modeling. *Biotechniques.* 1993;14(6):1010-1013.
  38. Gasteiger J, Marsili M. Iterative partial equalization of orbital electronegativity-a rapid access to atomic charges. *Tetrahedron.* 1980;36(22):3219-3228.
  39. Wolber G, Dornhofer AA, Langer T. Efficient overlay of small organic molecules using 3D pharmacophores. *J Comp Aided Mol Des.* 2006;20(12):773-788.
  40. Humphrey W, Dalke A, Schulten K. VMD: Visual molecular dynamics. *J Mol Graph.* 1996;14(1):33-38.
  41. Van Der Spoel D, Lindahl E, Hess B, Groenhof G, Mark AE, Berendsen HJ. GROMACS: fast, flexible, and free. *J Comput Chem.* 2005;26(16):1701-1718.
  42. Berendsen HJC, Postma JPM, van Gunsteren W, DiNola A, Haak J. Molecular dynamics with coupling to an external bath. *J Chem Phys.* 1984;81:3684-3690.
  43. Parrinello M, Rahman A. Crystal structure and pair potentials: A molecular-dynamics study. *Phys Rev Lett.* 1980;45(4):1196-1198.
  44. Van Gunsteren WF, Berendsen H. A leap-frog algorithm for stochastic dynamics. *Mol Sim.* 1988;1(3):173-185.
  45. Sun Y, Wei S, Yin C, Liu L, Hu C, Zhao Y, *et al.* Synthesis and spectroscopic characterization of 4-butoxyethoxy-N-octadecyl-1, 8-naphthalimide as a new fluorescent probe for the determination of proteins. *Bioorg Med Chem Lett.* 2011;21(12):3798-3804.
  46. Wang Q, Sun Q, Tang P, Tang B, He J, Ma X, *et al.* Determination of potential main sites of apixaban binding in human serum albumin by combined spectroscopic and docking investigations. *RSC Adv.* 2015;5(99):81696-81706.
  47. Borgå O, Borgå B. Serum protein binding of nonsteroidal antiinflammatory drugs: a comparative study. *J Pharmacokinet Biopharm.* 1997;25(1):63-77.
  48. Ghalandari B, Divsalar A, Saboury AA, Haertlé T, Parivar K, Bazl R, *et al.* Spectroscopic and theoretical investigation of oxali-palladium interactions with  $\beta$ -lactoglobulin. *Spectrochim Acta A Mol Biomol Spectrosc.* 2014;118:1038-1046.
  49. Mahdiuni H, Bijari N, Varzandian M, Ghadami SA, Khazaei M, Nikbakht MR, *et al.* Appraisal of sildenafil binding on the structure and promiscuous esterase activity of native and histidine-modified forms of carbonic anhydrase II. *Biophys Chem.* 2013;175-176:1-16.
  50. Brodersen R, Andersen S, Vorum H, Nielsen SU, Pedersen AO. Multiple fatty acid binding to albumin in human blood plasma. *Eur J Biochem.* 1990;189(2):343-349.
  51. Sudlow G, Birkett DJ, Wade DN. Further characterization of specific drug binding sites on human serum albumin. *Mol Pharmacol.* 1976;12(6):1052-1061.